

Received: 17 October 2020, Accepted: 23 February 2021

Edited by: R. Cerbino

Reviewed by: F. Giavazzi, Università degli Studi di Milano, Italy

Licence: Creative Commons Attribution 4.0

DOI: <https://doi.org/10.4279/PIP.130002>

ISSN 1852-4249

Radial percolation reveals that Cancer Stem Cells are trapped in the core of colonies

Lucas Barberis^{1*}

Using geometrical arguments, it is shown that Cancer Stem Cells (CSCs) must be confined inside solid tumors under natural conditions. Aided by an agent-based model and percolation theory, the probability of a CSC being positioned at the border of a colony is estimated. This probability is estimated as a function of the CSC self-renewal probability p_s ; i.e., the chance that a CSC remains undifferentiated after mitosis. In the most common situations p_s is low, and most CSCs produce differentiated cells at a very low rate. The results presented here show that CSCs form a small core in the center of a cancer cell colony; they become quiescent due to the lack of space to proliferate, which stabilizes their population size. This result provides a simple explanation for the CSC niche size, dispensing with the need for quorum sensing or other proposed signaling mechanisms. It also supports the hypothesis that metastases are likely to start at the very beginning of tumor development.

I Introduction

Cancer Stem Cells (CSCs) are responsible for driving tumor growth due to their ability to make copies of themselves (self-renewal) and differentiate into cells with more specific functions [1]. Differentiated Cancer Cells (DCCs) maintain a limited ability to proliferate, but can only generate cells of their specific lineage [2].

Like the tissues from which they arise, solid tumors are composed of a heterogeneous population of cells; many properties of normal stem cells are shared by at least a subset of cancer cells [3,4]. In many tissues, normal stem cells must be able to migrate to different regions of an organ, where they give rise to the specifically differentiated cells required by the organism. These features

are reminiscent of invasion and immortality, two hallmark properties of cancer cells [5, 6]. Resistance to chemo/radio therapies gives the CSCs a high chance of survival and of forming new tumors, even after treatment [7]. Hence, based on the concept that destroying or incapacitating CSCs would be an efficient method of cancer containment and control, new therapeutic paradigms are the focus of current research.

A *tumorsphere assay* is an experimental biological model used for the study of CSC features. A tumorsphere is a clonal aggregate of cancer cells grown *in vitro* from a single cell. It has been shown experimentally that DCCs can not generate a tumorsphere because they are unable to form compact long-term aggregates. As a consequence, the current experimental convention for the definition of CSCs, from a functional point of view, is based on the capacity of a single cell, the *seed*, to grow a more or less spherical aggregate in a gel suspension. This is why CSCs are said to “drive” tumor progression.

*lbarberis@unc.edu.ar

¹ Instituto de Física Enrique Gaviola (IFEG) and Facultad de Matemática, Astronomía, Física y Computación, CONICET and UNC, X5000HUE Córdoba, Argentina.

In an experimental assay, where the time evolution of the number of cells in a tumorsphere is measured, it is possible to determine a proliferation rate r consistent with the *Population Doubling Time* (PDT) of the total population. Unfortunately, this quantity cannot discriminate between the growth rates of CSCs and their differentiated counterparts. Furthermore, measuring the PDT of the CSCs is experimentally very complex [8]. Understanding r is crucial for mathematical modeling in a system where the offspring might belong to a different population than their parents. Indeed, CSC duplication could have three possible outcomes: stem cell replication (self-renewal), asymmetric differentiation and symmetric differentiation. To model such a feature mathematically, we can assume that the three outcomes will occur with probabilities p_s , p_a and p_d , respectively. From the point of view of the populations, the last two possibilities correspond to the birth of a new DCC, the parent cell either keeping (in the asymmetric duplication) or losing (in the symmetric case) its stemness. For example, writing the corresponding population dynamics differential equations, Benítez *et al.* showed that a CSC will give birth to another CSC at a rate rp_s which is estimated by fitting their mathematical model to the experimental data [9,10]. Since the probability of self-replication p_s seems to be small in homeostasis and in most common culture media, then rp_s will also be small, leading to *quiescence*, a main feature of CSCs. Nevertheless, CSCs can be experimentally forced to abandon their quiescent state by using specific growth factors that inhibit differentiation [11,12] or by restricting oxygen concentration, as discussed below. In these situations, p_s is close to one and tumorspheres will contain a high fraction of CSCs. Also, p_a is usually small, although its value can increase under abnormal situations such as injury or disease.

Metastasis, the invasion process by which cancer cells leave a tumor to form a new colony at another location, is an intriguing feature of cancer disease. Because CSCs are the seeds of tumors, it is accepted that metastatic tumors must come from a pre-existent *primary* tumor and might be located near its surface in order to detach, migrate and finally invade another site in the organism.

The distribution of CSCs in a primary tumor is key to the understanding of metastasis, cell proliferation and drug resistance. Curiously, according to

the three-concentric-layer model proposed by Persano *et al.*, CSCs seem to be located in the inner core of glioblastomas. On the other hand, cells on the periphery of the tumor show a more differentiated phenotype that is highly sensitive to Temozolomide, a drug for cancer treatment [13]. Interestingly, these authors demonstrate that CSCs are more proliferative under hypoxic conditions. Furthermore, Li *et al.* report that hypoxia plays an important role in the de-differentiation of cells [14]. These results indicate that a hypoxic environment will increase the numbers of CSCs.

The aim of this work is to simulate colony growth by means of an Agent-Based Model (ABM) that mimics basic features of CSC proliferation, with emphasis on its geometrical properties. Multiple realizations allow us to estimate the fraction of CSCs situated on the periphery of the colony, showing that it is quite small for large, long-lived colonies. We also use some elements of percolation theory to help interpret and quantify the simulation results. We then report a transition to percolation which depends on the self-renewal probability, p_s , of the CSC population. Finally, we conclude that that our results lead to a simple explanation for CSC niche size, and support the hypothesis that the metastatic process must start at the very beginning of tumor development.

II Simulation of two-dimensional colonies

Experimental monoclonal colonies start with a CSC in a suitable culture medium. This cell and its daughters duplicate at a more or less constant rate, forming a colony with an approximately circular shape. The reader interested in examples may refer to [15–17] for further information. In this work we use the same principle, describing the cells using circle-shaped mathematical objects and refining rules for their duplication and movement. In later studies we will require cells not to be rigid spheres. Each cell in the current simulations has a central circular impenetrable region, the *core*, and around the core there is an area, the *corona*, where overlapping is allowed. In this way, cells are able to overlap as far as the border of their coronas and reach the border of the core of other, neighboring cells. The figures presented in this work has a 95 % overlap

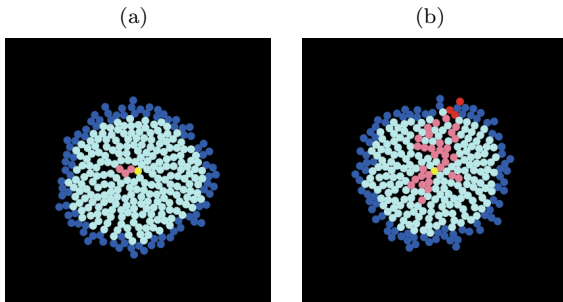


Figure 1: Two realizations of the simulation for $p_s = 0.5$ after 15 days. (a) There are no CSCs at the periphery; all of them, colored in pink, became quiescent. (b) The active CSCs at the border are colored in red. Note that some branches failed to percolate. DCCs are depicted in cyan (quiescent) and blue (active). The seed is represented in yellow.

on the cell radius. However, we will show that the results presented here do not depend on this parameter. Also, each cell belongs to a class that defines its behavior: active CSCs, active DCCs, quiescent CSCs and quiescent DCCs. As a simplification of the model, we assume that the probability of asymmetric duplication of CSCs is zero, $p_a = 0$. In this way p_s is the only control parameter that allows direct capture of the model's main features.

We start the simulation by seeding an active CSC and asking it to duplicate. Furthermore, at each time step we ask all active cells to attempt to duplicate, according to the following rules. First a new cell is created in a random position at the side of an active cell. If there are no other cells in this location it remains there, otherwise a new location beside the active cell is randomly determined. After 500 attempts, if the new cell has still not found an empty spot to occupy, it is destroyed and the active cell changes to its respective quiescent class. Conversely, after successful duplication, if the active cell is a CSC it self-renews with a probability p_s , which means that the new cell becomes an active CSC, otherwise it changes to the active DCC class. If the new, active cells belong to different classes, there is a probability of $1/2$ that the active CSC will exchange positions with the new DCC. Naturally, an active DCC can only create another DCC.

Once all the active cells have been asked to duplicate, independently of the success of the attempt

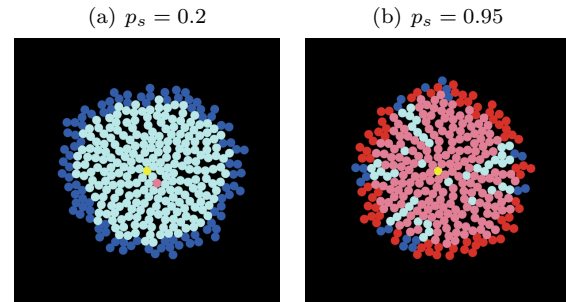


Figure 2: Two realizations of the simulation at low (a) and high (b) self-replication rates after 15 days. In (a) the CSCs are quickly surrounded by DCCs, becoming quiescent (pink). In (b) the high number of CSCs allows percolation to most of the colony perimeter. The seed is colored in yellow.

we say that a one-day-long time step has been performed. This implies, without loss of generality, that $r \simeq 1 \text{ day}^{-1}$, a reasonable growth rate that will aid our intuition. Further details on the structure of the simulation process are provided in the Appendix, including a flow chart in Fig. 7. We have also provided videos in the Supplementary Information. In each video a representative value of p_s was set and ten realizations were recorded, illustrating how they were carried out.

Typical outcomes of the described process are shown in Fig. 1 and video v1. In these examples we set $p_s = 0.5$ and started with a CSC seed depicted in yellow. After running the simulation for a period equivalent to two weeks (15 time steps), a relatively long period for a biological experiment, we obtained two possible outcomes: (a) a few quiescent CSCs were trapped in the center of the colony or (b) there were active CSCs at the border of the colony. Indeed, we defined the *border* of the colony as the rim formed by the set of active cells. To better track the subpopulations present in the colony, the active cells are colored in red for CSC and in blue for DCC. Also, the quiescent cells are colored in pink for CSC and cyan for DCC. Remember that the yellow dot is not always at the center of the colony because the seed may exchange its position with a new DCC. In panel (b) we recognize a path, paved by CSCs, that joins the center of the colony with its border. Also, some frustrated branches appear in this path of CSCs, which die in the quiescent core, indicating great variability. This path resembles

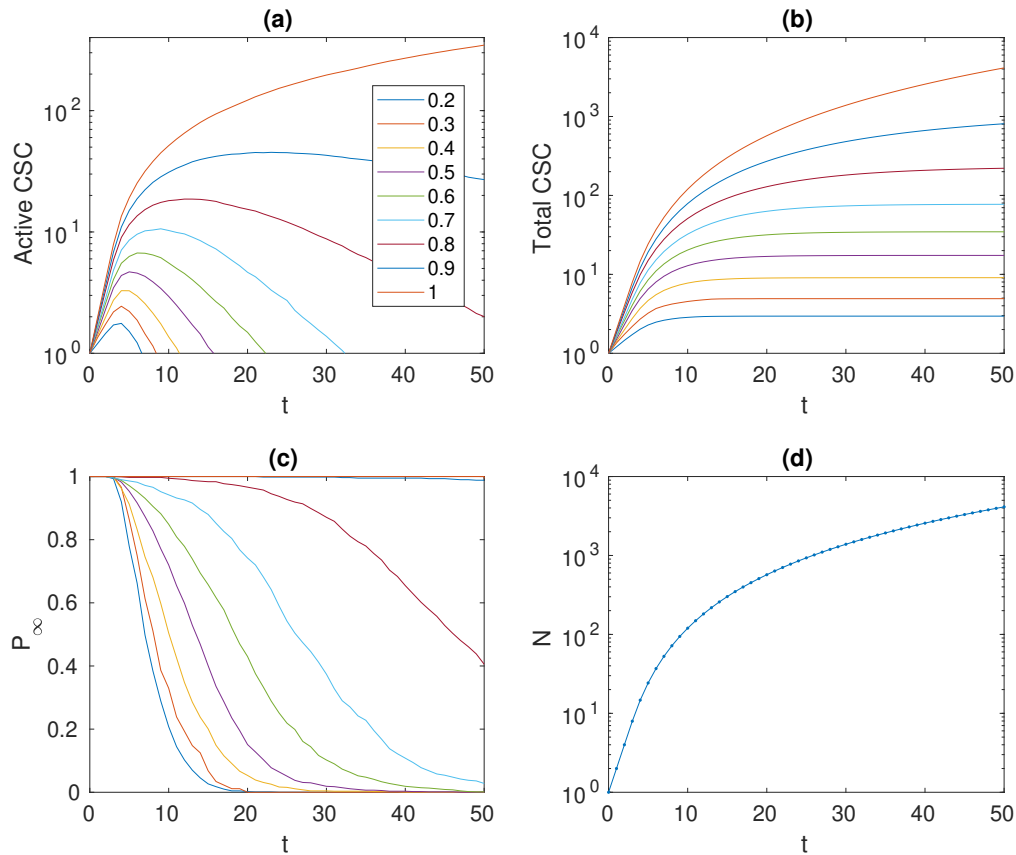


Figure 3: Time evolutions of quantities averaged over a thousand realizations for values of $p_s \in [0.2..1.0]$. (a) Number of CSCs at the border. (b) The total number of CSCs reaches a constant value that defines the niche. (c) The probability of a CSC being at the border. (d) System size as a function of time.

cluster percolation in porous media, lattices or networks, which led to us to attempt to describe the probability of finding a CSC at the border of the colony by means of percolation theory.

To sharpen our intuition as to what percolation means in this system, in Fig. 2 and videos v2 and v3 we present two more examples with different self-replication probabilities, p_s . In panel (a) and video v2, $p_s = 0.2$ is so small that the CSCs are quickly surrounded by DCCs, and become quiescent. This is the most common situation in a regular culture medium where the CSC count is low and constant —over time. On the other hand, in panel (b) and video v3, $p_s = 0.95$ leads to a large CSC population that invades almost the entire system. The addition of stem cell maintenance factors such as EGF or bFGF to the culture medium is an example of this case. These limiting situations were

previously studied both experimentally [11,18] and mathematically [9,10], focusing in the first case on technical aspects of the assay, and in the second case on recovery of the CSC fraction.

Curiously, in the examples shown in Figs. 1 and 2, the rim formed by active cells is similar to the one reported in the classical multicellular spheroid work of Freyer and Shuterland [19]. In Freyer's work, the inner portion of the spheroids was formed by dead cells, attributed to a low concentration of oxygen/nutrients supplied by means of diffusion. This rim was also formed by active cells and was studied mathematically by several authors using diffusion equations [20–22]. It is interesting that in the present monoclonal case the geometry seems to be sufficient to develop a rim, just two cells thick, independently of any diffusion process.

To study the percolation properties of the system statistically, we carried out extensive simulations of colony growth. Each data point reported is the result of averaging over 1000 runs. The time evolution of colony growth was performed for 37 values of $p_s \in [0.2, 1.0]$. The results of these measurements are summarized in Fig. 3. Panel (a) shows the number of CSCs at the border, which increases to a maximum given by the time when they are overwhelmed by the DCC population. Beyond this point, more and more CSCs become quiescent until no more active CSCs remain. This phenomenon disappears for p_s barely lower than 1, when almost all cells on the border are CSCs. In panel (b) the time evolution of the total CSC population is depicted, showing that after a transient the CSC population stops growing and remains constant. This fixed number of CSCs is usually called the *CSC niche* and was mathematically studied in [9]. As expected, the probability of a CSC being at the border rises as p_s is increased, as shown in panel (c). The relationship between simulation time and system size is shown in panel (d); due to its geometrical nature it is independent of p_s , the self-renewal probability.

III Percolation theory

Percolation theory was used to estimate the probability of finding a CSC at the border of the colony, looking for a purely geometrical feature of its growth. In particular, we assumed that the cells in the colony could be mapped onto the nodes of a triangular network with the seed at its center. Each cell is then connected with its nearest neighbors, whose number, in two dimensions, is known not to exceed six. As shown in Fig. 1(b), the CSCs (quiescent and active) form *paths* that expand radially from the center to the edge of the colony. By inspection, we note that these paths are formed by the connected nodes that have had a CSC at any moment during the culture. The path could have some “holes” that arise because of the possibility of exchanging a parent CSC with its daughter DCC. The probability p_s thus regulates the number of CSCs that occupy the nodes of the network. Hence, there must be a threshold value p_c of p_s , below which it is impossible to follow a path of nodes starting at the seed and ending in a CSC at the

border of the tumor. This value, p_c , is called the *critical value* or *percolation threshold* and defines a *percolation phase transition*[23]. Thus, when the border is reached by CSCs, we say that such a path *percolates*.

Formally, a percolating path is mathematically defined as a set of connected nodes that expands infinitely over an infinite network for a large enough value of p_s [24]. In our model, each new node of the percolation path is added either by the self-renewal of a CSC, with probability p_s , or by an exchange between a CSC and a DCC, with probability $\frac{1}{2} \times (1 - p_s)$, after a CSC gives birth to a DCC. It is also important to note that several neighboring nodes could already be occupied. Thus, it is useful to define the *average empty neighbor number* z as follows: Imagine that we perform a random walk starting at the seed’s node along an infinite path where it is forbidden to step back. At each step there are z branches in the network, but there is also a probability $p_s + \frac{1 - p_s}{2}$ that a node belongs to the path, so on average only $\frac{1}{2}(p_s + 1)z$ will be accessible. To continue walking along the path, there must be at least one empty node to walk along, leading to the condition $\frac{1}{2}(p_s + 1)z \geq 1$. Therefore, the *critical probability* for transition to percolation is

$$p_c = \frac{2}{z} - 1, \quad (1)$$

which depends on the available neighbor number. ¹ It is noteworthy that in Eq. (1), for $z = 1$ we obtain $p_c = 1$, the 1D critical occupation for a chain of nodes. For $1 < z < 2$ the critical occupation quickly falls to zero. This means that for $z \geq 2$ the system will always percolate. On the other hand, if the CSC never exchanges its position with a DCC, we get $p_c = \frac{1}{z}$, which is again the 1D critical occupation and will asymptotically fall to zero as z increases. Otherwise, if the CSC always moves, p_s diverges as expected for a cell that always remains on the outer rim of the growing colony. There is no evidence that a CSC will stay either in the core or on the border of the colony. Simulations carried out on both limits of the exchange probability agree with these theoretical limits, but do not provide further information. For this reason, we implemented the one-half exchange probability in our

¹Remember it is not universal because it depends on the details of the network.

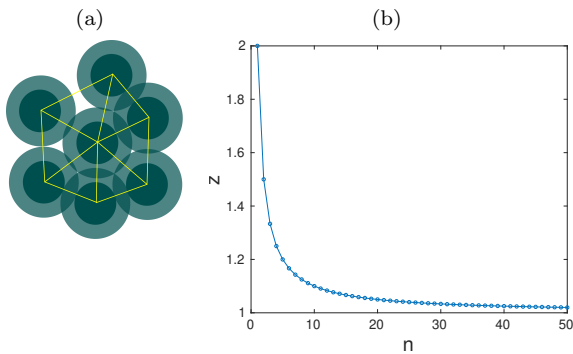


Figure 4: (a) Cell overlapping does not change the maximum neighbor number of six; thus, the underlying lattice is topologically triangular (yellow lines). (b) The average neighbor number versus layer number quickly drops to one. At $t = 50$ days, $n \simeq 50$, $N \simeq 4000$ and $z = 1.02$, which means $p_s = 0.92$.

simulations, using the “*a priori* equal probability” principle.

By construction, there are no closed loops in the network, thus deduction of the critical probability was similar to that for a Bethe lattice or a tree graph. However, unlike regular lattices/graphs, in our model the neighbor number of a node is not the same for all nodes due the randomness introduced by space searching and the probability of exchange. For this reason, we defined an average neighbor number. In Fig. 4(a) each cell is depicted by two concentric circles; the dark one represents the rigid core and the lighter represents the corona where overlapping is allowed. Note that the maximum neighbor number is six, regardless of the extent of the corona. In simulations a new cell must be in contact with other cells, and overlapping will modify the density of the colony. As mentioned, this parameter will be useful for further study of diffusion effects that are irrelevant to the present work. Also, the random process of searching space for proliferation will slightly modify the geometry of the underlying network, but not its topology, which will be the same as that of the triangular lattice except for a few defects caused by a neighbor number lower than six. Thus density, which is relevant when studying the diffusion of nutrients, oxygen or proteins for signaling, does not play any role in the current percolation problem.

To roughly estimate z we built up a tree graph

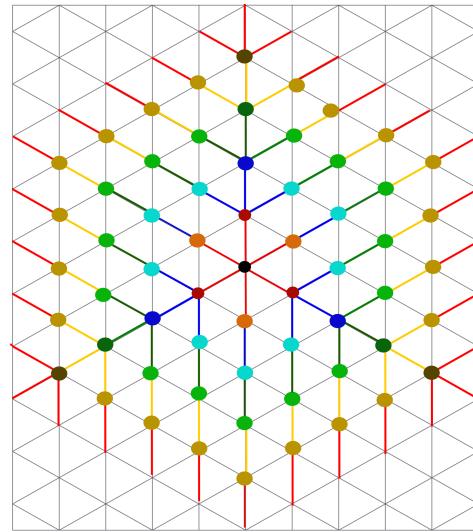


Figure 5: Growth of the colony on a triangular lattice, starting from the center (black dot). Each layer is depicted in a different color and contains three nodes with $z = 3$ and the remainder with $z = 1$.

over a triangular lattice substrate. A possible connection pattern of nodes in such a network is depicted in Fig. 5, which was built layer by layer with each layer represented in a different color. Layer $n = 0$ is the central black dot that represents the seed. In this particular example, in each layer we depict three nodes with $z = 3$ (darker dots), leaving the remaining nodes with $z = 1$ (lighter dots). It is clear that for any layer there are $6 \times n$ nodes for $n > 0$; then to connect two layers without loops we need on average $z = \frac{n+1}{n}$. Because $1 < z < 2$ quickly decays with n , c.f. Fig. 4(b), we do expect that the critical probability for percolation, given by Eq. (1), will shift to $p_c = \frac{n}{n+1} \rightarrow 1$ as $n \rightarrow \infty$. The size of the network will be $N = 6 \sum_{i=1}^n i + 1$ leading to the limit $p_c \xrightarrow{N \rightarrow \infty} 1$. Thus, as the colony increases in size, the percolation threshold shifts towards 1. The main consequence is that there is no chance to perform finite size scaling to detect the critical transition point through simulations, as in the case of 1D chains.

As mentioned before, in Figs. 1 and 2, the proliferative cells are distributed in the two outermost layers. This feature of the colony occurs because the cells in the simulation are requested to proliferate in random order. This is also the cause of

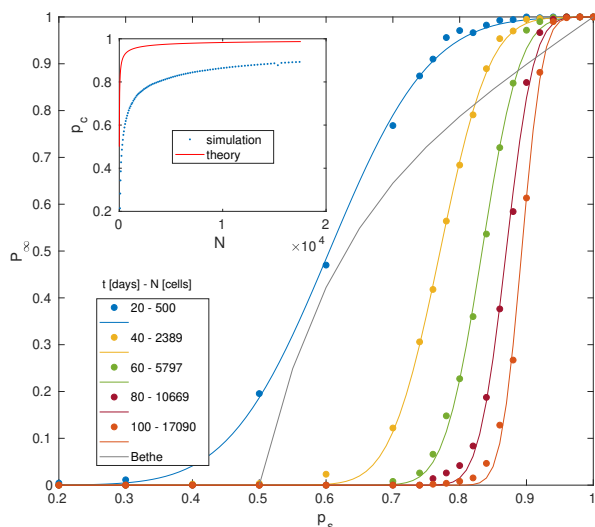


Figure 6: Probability of percolation as a function of p_s for different colony sizes. Dots correspond to simulations and lines are theoretical fittings to estimate the percolation threshold (see text). The gray line is the theoretical Bethe result. Inset: Percolation threshold p_c at different sizes measured by simulations (blue). Our simple theoretical approach overestimates this threshold (red).

the observed circular shape of the colony. Because the vertices of the hexagonal array shown in Fig. 5 have a lower probability of being chosen for proliferation, as system size increases cells on their edges will proliferate first, as at the beginning of each time step they have more room to do so. Thus, the estimated number of cells in each layer is underestimated, as is their neighbor number. As a consequence, we expect that the actual value of p_c as a function of size or time will be much lower than that predicted by Eq. (1) and our estimation of z . A precise estimation of z will require statistical treatment that is beyond the scope of this article.

The result implies that proper (mathematical) percolation transition will occur at $p_s = 1$, as in 1D percolation. This also implies that the only way for a CSC to be at the border, for an arbitrarily large colony, is when it is forced not to differentiate. Nevertheless, monoclonal colonies cannot be maintained and grown forever. A 50-day experiment is very long, and very uncommon in the literature.

We thus focus on the probability of a CSC being at the border, P_∞ , whose behavior, as a function

of p_s , is depicted in Fig. 6 for several times/sizes. The relationship between time and size is bijective, thus we report both values in the legend. In this graph the dots are the result of the simulations presented in the previous section, for which the frequency of CSCs at the border of the colony was averaged over a thousand runs. To obtain suitable fitting of these data as continuous functions of p_s , we used erf functions following Yonezawa's classical work [23]. The inflection point of the erf curves coincides with the percolation threshold, giving a good estimate of p_c . In addition, the theoretical result for the percolation parameter in a Bethe lattice of order 3 is depicted in gray for comparative purposes. Note that P_∞ does not jump as in Bethe percolation; the transition is continuous, as known for several regular lattices, including the triangular one. Gonzalez *et al.* [25] studied the transitions of several forms of percolation in triangular lattices, reporting their critical probabilities using finite size scaling analysis. They found universal features with values between 0.5 and 0.8 for the percolation threshold, depending on the problem. In contrast, but as expected, as our system size increases the fitted curves become steeper and steeper, and their inflection points predict a shift of p_s towards 1, as depicted by the blue dots in the inset of Fig. 6. Comparison with our theoretical result gives an expected overestimation of the percolation threshold – the red line, as explained before. We therefore hope to find that a CSC will be at the border of the colony in half the runs when we simulate a three-week experiment.

IV Conclusions

Metastasis is an intriguing feature of cancer invasion. Most research in this field is guided by the biological point of view, even though there are many mathematical models that attempt to describe it [26–29].

In the examples of growth given in Fig. 1(a) and Fig. 2(a), it becomes clear that under normal culture conditions CSCs remain in the inner core of spheroids. This is also deduced from the low P_∞ probability of finding a CSC at the border of the colony, as shown in Fig. 6. If this could be observed in the laboratory, the experiments that reveal a CSC preference for hypoxic environments could be

easily explained by this fact. It has been shown experimentally that hypoxia maintains the undifferentiated state of primary glioma cells, slowing down the growth of glioma cells which are in a relatively quiescent stage, increasing colony-forming efficiency and the migration of glioma cells, and elevating the expression of stem cell markers. However, the expression of markers for stem cell differentiation was reduced after hypoxia treatment [13, 14]. It is also known that the inner core of spheroids and tumors have a lack of oxygen and nutrients, which are first consumed by the outer layers of the tumor [30–33]. In this context, CSCs constitute a phenotype that has evolved to survive under hypoxic conditions in order to drive tumor growth.

On the other hand, metastasis requires CSCs to overcome three major barriers: the probability of an active CSC being present at the border of the colony, the probability of it detaching from the tumor and the probability of it finding a suitable place to proliferate. The results of the present work establish that the first of these probabilities is very small, even for relatively small tumors, supporting the rare occurrence of metastasis.

For large self-replication rates, possibly generated by environmental conditions, many active CSCs would become candidates for detachment. At present, we do not know of any report of a high number of CSCs in tumors *in vivo* or in transplanted xenographs under normal physiological conditions that experimentally support a large self-replication rate as part of the metastasis mechanism.

An intriguing possibility is that metastasis begins in the early stages of tumor progression [34–36]. This is deduced from Fig. 3(a) where the number of active CSCs shows a peak for low p_s and short times. If this is the actual situation, a CSC must detach from the primary tumor in its first week of life, when the probability of being at the border is close to 1, even for low values of self-replication. Note that at this time the tumor consists of no more than a dozen cells. This fact leads us to hypothesize that a primary tumor is indeed the metastasis of some small young tumors. According to this hypothesis the primary tumor is in fact the first colony able to fix and grow, while metastatic tumors come from later CSCs that take more time to attach successfully to a new location. The de-

tached cells must survive while competing for nutrients and space with the primary spheroids, which at this stage are ruthless adversaries [37].

Our two-dimensional model could be extended to three dimensions; this would be more realistic but also computationally more expensive. Preliminary results are qualitatively similar to those reported here, but so far we lack the statistics to perform a quantitative comparison. Another feature, obtained by changing geometrical constraints in our code, are simulations of non-solid tumors such as haematologic neoplasm; preliminary results show that active CSCs are present in a larger proportion there than in solid tumor spheroids. As a consequence, there is a higher probability of CSCs detaching and developing metastasis in neoplasms.

In summary, percolation provides a way of developing a geometrical theory to support or complement signaling pathways, quorum sensing and other tools frequently used to study metastasis. Further experimental research will elucidate whether CSCs are the survivors with greatest fitness, as suggested by our present results.

Acknowledgements - This work was supported by SECyT-UNC (project 05/B457) and CONICET (PIP 11220150100644), Argentina. The author is grateful to Dr. C. A. Condat and Dr. L. Vellón for fruitful discussions. Also, he thanks Dr. Fabio Giavazzi for suggesting a better approach for Eq. (1).

Appendix: Simulation algorithm.

The simulations were carried out in an object-oriented paradigm. Each cell belongs to one of the following classes: Active CSC, active DCC, quiescent CSC or quiescent CSC. First we created an active CSC object at the center of a square space large enough to contain the final colony. Then for each time step we requested, in random order, that all objects belonging to an active class perform the duplication procedure. In the left-hand column of Fig. 7 we depict the flow chart of the duplication procedure, whose steps are illustrated in the right-hand column.

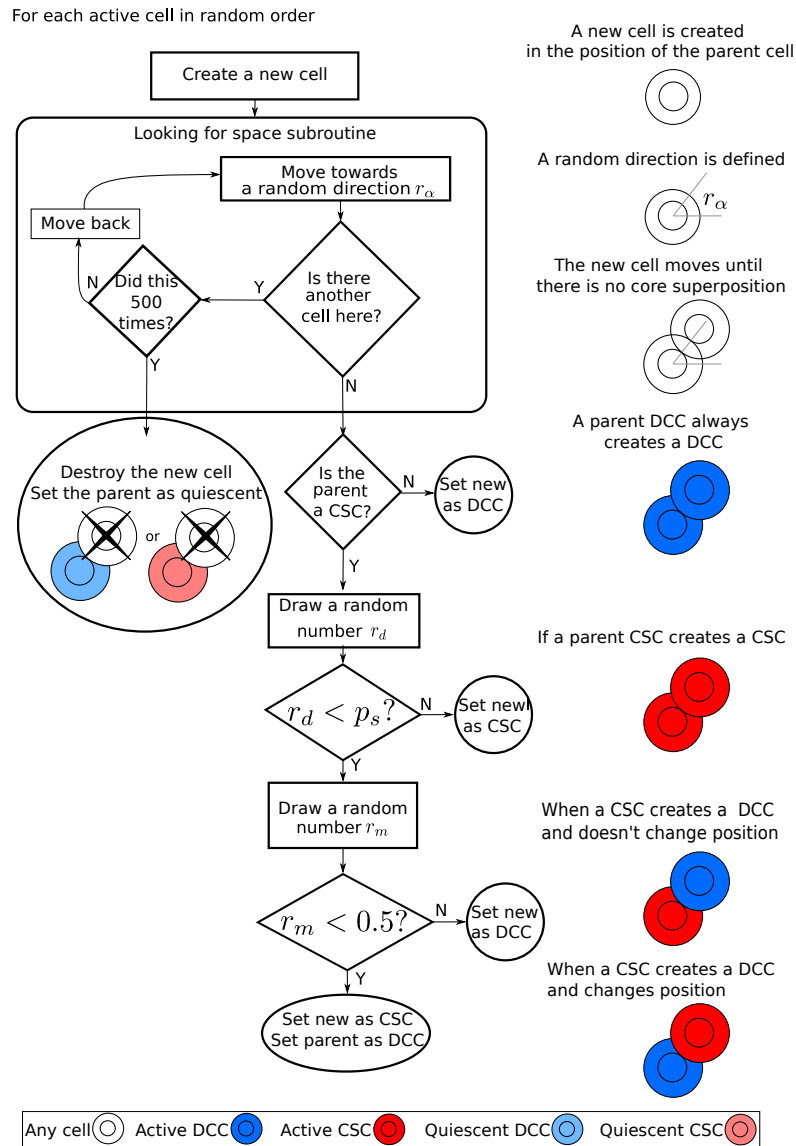


Figure 7: Left: Flow chart for the proliferation process of each cell. Right: Illustration of the stages and outcomes of the duplication process.

The duplication process starts when an active cell, the *parent*, creates a copy of itself, the *new* cell, in the same position. Then a random angle $0 \leq r_\alpha < 2\pi$ is drawn from a uniform distribution and the new cell will advance a certain distance in the direction defined by this angle, such that its border does not overlap with its parent's core. This distance was determined as 95% of the cell diameter. If in its new position the border of the new cell

overlaps with the core of another cell, it moves back to its initial position. Another random direction is then defined, repeating the movement sequence. The new cell will move forward and back, randomly changing its direction until there is no overlapping; thus we say that an empty spot is found. After 500 failed attempts to find an empty spot, the new cell is destroyed and the parent cell changes to its respective quiescent class. Conversely, if the new cell

finds an empty spot, and if its parent is a DCC, it sets its own class as an active DCC. On the other hand, if the parent is a CSC, a new random number $0 \leq r_d < 1$ is drawn to be compared with p_s . If $r_d < p_s$ the new cell will set its class to active CSC, otherwise the new cell class will be set to active DCC. In the latter case a new random number $1 \leq r_m < 1$ is drawn, and if the comparison $r_m < 1/2$ becomes true, the cells will exchange their positions, leaving the CSC in the new spot and the DCC in the position of its parent.

Note that quiescent cells will never be requested to do anything; they do not move or duplicate in these simulations. Their only role is to restrict the movement of active cells. As a consequence, the code runs very rapidly, even for large colonies.

-
- [1] E Batlle, H Clevers, *Cancer stem cells revisited*, *Nat. Med.* **23**, 1124 (2017).
- [2] C A M La Porta, S Zapperi, J P Sethna, *Senescent cells in growing tumors: Population dynamics and cancer stem cells*, *PLoS Comput. Biol.* **8**, e1002316 (2012).
- [3] N A Lobo, Y Shimono, D Qian, M F Clarke, *The biology of cancer stem cells*, *Annu. Rev. Cell Dev. Biol.* **23**, 675 (2007).
- [4] J Stingl, C Caldas, *Molecular heterogeneity of breast carcinomas and the cancer stem cell hypothesis*, *Nat. Rev. Cancer* **7**, 791 (2007).
- [5] Y Shimono, M Zabala, R W Cho, N Lobo, P Dalerba, D Qian, M Diehn, H Liu, S P Panula, E Chiao, F M Dirbas, G Somlo, R A Reijo Pera, K Lao, M F Clarke, *Downregulation of miRNA-200c links breast cancer stem cells with normal stem cells*, *Cell* **138**, 592 (2009).
- [6] D Hanahan, R A Weinberg, *The hallmarks of cancer review*, *Cell* **100**, 57 (2000).
- [7] P Jagust, B de Luxán-Delgado, B Parejo-Alonso, P Sancho, *Metabolism-based therapeutic strategies targeting cancer stem cells*, *Front. Pharmacol.* **10**, 203 (2019).
- [8] A Waisman, F Sevlever, M Elías Costa, M S Cosentino, S G Miriuka, A C Ventura, A S Guberman, *Cell cycle dynamics of mouse embryonic stem cells in the ground state and during transition to formative pluripotency*, *Sci. Rep* **9**, 8051 (2019).
- [9] L Benítez, L Barberis, C A Condat, *Modeling tumorspheres reveals cancer stem cell niche building and plasticity*, *Physica A* **533**, 121906 (2019).
- [10] L Benítez, L Barberis, C A Condat, *Understanding the influence of substrate when growing tumorspheres*, *BMC Cancer (In press)* (2021).
- [11] J Wang, X Liu, Z Jiang, L Li, Z Cui, Y Gao, D Kong, X Liu, *A novel method to limit breast cancer stem cells in states of quiescence, proliferation or differentiation: Use of gel stress in combination with stem cell growth factors*, *Oncol. Lett.* **12**, 1355 (2016).
- [12] Y C Chen, P N Ingram, S Fouladdel, S P McDermott, E Azizi, M S Wicha, E Yoon, *High-throughput single-cell derived sphere formation for cancer stem-like cell identification and analysis*, *Sci. Rep.* **6**, 27301 (2016).
- [13] L Persano, E Rampazzo, A Della Puppa, F Pistollato, G Basso, *The three-layer concentric model of glioblastoma: Cancer stem cells, microenvironmental regulation, and therapeutic implications*, *TheScientificWorldJo.* **11**, 1829 (2011).
- [14] P Li, C Zhou, L Xu, H Xiao, *Hypoxia enhances stemness of cancer stem cells in glioblastoma: An in vitro study*, *Int. J. Med. Sci.* **10**, 399 (2013).
- [15] C Zhang, Y Tian, F Song, C Fu, B Han, Y Wang, *Salinomycin inhibits the growth of colorectal carcinoma by targeting tumor stem cells*, *Oncol. Rep.* **34**, 2469 (2015).
- [16] S Shankar, D Nall, S-N Tang, D Meeker, J Passarini, J SharmaR, K Srivastava, *Resveratrol inhibits pancreatic cancer stem cell characteristics in human and Kras^{G12D} transgenic mice by inhibiting pluripotency maintaining factors and epithelial-mesenchymal transition*, *PLoS ONE* **6**, e16530 (2011).

- [17] A Schneider, D Spitkovsky, P Riess, M Molcanyi, N Kamiseti, M Maegele, J Hescheler, U Schaefer, “*The good into the pot, the bad into the crop!*” — *A new technology to free stem cells from feeder cells*, *PLoS ONE* **3**, e3788 (2008).
- [18] A Chen, L Wang, S Liu, Y Wang, Y Liu, M Wang, *Attraction and compaction of migratory breast cancer cells by bone matrix proteins through tumor-osteocyte interactions*, *Sci. Rep.* **8**, 5420 (2018).
- [19] J P Freyer, R M Sutherland, Regulation of growth saturation and development of necrosis in EMT6/Ro multicellular spheroids by the glucose and oxygen supply, *Cancer Res.* **46**, 3504 (1986).
- [20] C A Condat, S A Menchón, *Ontogenetic growth of multicellular tumor spheroids*, *Physica A* **371**, 76 (2006).
- [21] S A Menchón, C A Condat, *Cancer growth: Predictions of a realistic model*, *Phys. Rev. E* **78**, 022901 (2008).
- [22] L Barberis, C A Condat, *Describing interactive growth using vector universalities*, *Ecol. Model.* **227**, 56 (2012).
- [23] F Yonezawa, S Sakamoto, M Hori, *Percolation in two-dimensional lattices. I. A technique for the estimation of thresholds*, *Phys. Rev. B* **40**, 636 (1989).
- [24] K Christensen, N R Moloney, *Complexity and Criticality*, Imperial College Press, London, UK (2005).
- [25] M I González, P Centres, W Lebrecht, A J Ramirez-Pastor, F Nieto, *Site-bond percolation on triangular lattices: Monte Carlo simulation and analytical approach*, *Physica A* **392**, 6330 (2013).
- [26] K Iwata, K Kawasaki, N Shigesada, *A dynamical model for the growth and size distribution of multiple metastatic tumors*, *J. Theor. Biol.* **203**, 177 (2000).
- [27] S A Menchón, C A Condat, *Modeling tumor cell shedding*, *Eur. Biophys. J.* **38**, 479 (2009).
- [28] J B McGillen, E A Gaffney, N K Martin, P K Maini, *A general reaction-diffusion model of acidity in cancer invasion*, *J. of Math. Biol.* **68**, 1199 (2014).
- [29] A Rhodes, T Hillen, *A mathematical model for the immune-mediated theory of metastasis*, *J. Theor. Biol.* **482**, 109999 (2019).
- [30] A I Liapis, G G Lipscomb, O K Crosser, E Tsiroyianni-Liapis, *A model of oxygen diffusion in absorbing tissue*, *Math. Modell.* **3**, 83 (1982).
- [31] P J Robinson, S I Rapoport, *Model for drug uptake by brain tumors: Effects of osmotic treatment and of diffusion in brain*, *J. Cerebr. Blood F. Met.* **10**, 153 (1990).
- [32] Y Jiang, J Pjesivac-Grbovic, C Cantrell, J P Freyer, *A multiscale model for avascular tumor growth*, *Biophys. J.* **89**, 3884 (2005).
- [33] J A Bull, F Mech, T Quaiser, S L Waters, H M Byrne, *Mathematical modelling reveals cellular dynamics within tumour spheroids*, *PLoS Comput. Biol.* **16**, e1007961 (2020).
- [34] J W Gray, *Evidence emerges for early metastasis and parallel evolution of primary and metastatic tumors*, *Cancer Cell* **4**, 4 (2003).
- [35] H Hosseini, M M Obradović, M Hoffmann, K L Harper, M S Sosa, M Werner-Klein, L K Nanduri, C Werno, C Ehrl, M Manneck, N Patwary, G Haunschild, M Gužvić, C Reimelt, M Grauvogl, N Eichner, F Weber, A D Hartkopf, F A Taran, S Y Brucker, T Fehm, B Rack, S Buchholz, R Spang, G Meister, J A Aguirre-Ghiso, C A Klein, *Early dissemination seeds metastasis in breast cancer*, *Nature* **540**, 552 (2016).
- [36] N Linde, M Casanova-Acebes, M S Sosa, A Mortha, A Rahman, E Farias, K Harper, E Tardio, I Reyes Torres, J Jones, J Condeelis, M Merad, J A Aguirre-Ghiso, *Macrophages orchestrate breast cancer early dissemination and metastasis*, *Nature Commun.* **9**, 1 (2018).
- [37] L Barberis, M A Pasquale, C A Condat, *Joint fitting reveals hidden interactions in tumor growth*, *J. Theor. Biol.* **365**, 420 (2015).